

Figure 12 Simulated and measured results of insertion loss and isolation of PIN diode SPDT switch

isolation path loss of 51–36 dB over a wide frequency range (2–18 GHz) have been measured. The close agreement obtained between the measured and simulated data is also shown. The total DC power consumption for this design is only around 1.2 mW for this switch.

4. CONCLUSIONS

Low insertion loss broadband PIN diode RF switches are implemented using a standard 0.18- μm SiGe process. By using the minimum ACD and octagonal geometry, the 50 μm^2 PIN diode can achieve 0.65 dB insertion loss, which is the best value reported for a standard 0.18- μm SiGe PIN diode with the same anode size. The measured OIP₃ of 23.4 dBm is well suited to the switching applications in phase array communication systems. The broadband (2–18 GHz) PIN diode SPDT switch through path demonstrated an insertion loss of 1.21–1.85 dB, while its isolation path shows an isolation of 51–36 dB while only consuming 1.2 mW of DC power. Integration of the developed PIN diode switches with other RF components is an attractive option for achieving highly integrated low cost SoC T/R modules in satellite and mobile applications.

REFERENCES

1. J.A. Torres and J.C. Freire, Monolithic transistors SPST switch for L-band, *IEEE Trans Microwave Theory Tech* 50 (2002), 51–56.
2. Y. Jin and C. Nguyen, Ultra-compact high-linearity high-power fully integrated DC- 20 GHz 0.18- μm CMOS T/R switch, *IEEE Trans Microwave Theory Tech* 55 (2007), 30–36.
3. R. Tayrani, M.A. Teshiba, G.M. Sakamoto, Q. Chaudhry, R. Alidid, Y. Kang, I.S. Ahmad, T.C. Cisco, M. Hauhe, Broad-band SiGe MMICs for phased- array radar applications, *IEEE J Solid-State Circuits* 38 (2003), 1462–1471.
4. P. Sun, P. Upadhyaya, D. Jeong, D. Heo, and G.S. La Rue, A novel SiGe PIN diode SPST switch for broadband T/R module, *Microwave Wireless Compon Lett* 17 (2006), 352–354.
5. B.A. Orner, Q. Liu, J. Johnson, R. Rassel, X. Liu, D. Sheridan, A. Joseph, and B. Gaucher, P-i-n diodes for monolithic millimeter wave BiCMOS applications, *Proc. 3rd Int SiGe Technology and Devices*, Princeton, USA, 2006.
6. R.H. Caverly and G. Hiller, Distortion in p-i-n diode control circuits, *IEEE Trans Microwave Theory Tech* 35 (1987), 492–501.
7. P. Sun, G. Wang, P. Liu, P. Upadhyaya, D. Jeong, and D. Heo, Silicon-based PIN SPST RF switches for improved linearity, In: *Proc IEEE MTT-S International Microwave Symposium*, Anaheim, USA, 2010.

8. P. Sun and D. Heo, Analysis of parasitic effects for PIN diode SPDT switch, *IEEE(IET) Electron Lett* 45 (2009), 503–504.
9. F. Hirose, K. Kurita, Y. Takahashi, and M. Mukaida, Operation mechanism on SiGe/Si/Si PIN diodes explained using numerical simulation, *Electrochem Solid State Lett* 8 (2005), 160–163.
10. P. Sun, P. Upadhyaya, L. Wang, D. Jeong, and D. Heo, High performance PIN diode in 0.18- μm SiGe BiCMOS process for broadband monolithic control circuits, *Proc. 1st European Microwave Integrated Circuits Conf.*, Manchester, UK, 2006, pp. 148–152.

© 2011 Wiley Periodicals, Inc.

POLARIZATION-PRESERVING EVANESCENT-MODE FILTERS

Seng Yong Yu and Jens Bornemann

Department of Electrical and Computer Engineering University of Victoria, Victoria, BC V8W 3P6, Canada; Corresponding author: j.bornemann@ieee.org

Received 23 August 2010

ABSTRACT: Rectangular and circular waveguide evanescent-mode filters with polarization-preserving properties are presented. The filters are formed by inserting quadruple-ridged resonators in a square or circular waveguide operated below cutoff. They are especially suited in applications requiring short and compact components. The numerical technique that facilitates eigenvalue and scattering parameter computations is verified against measurements. Basic design considerations are discussed, and structural dimensions are provided for two 9.5 GHz filters with 500 MHz bandwidth. Performances are validated by independent and commercially available electromagnetic software packages. Sensitivity issues for fabrication are addressed by a tolerance analysis. Fabrication accuracy is acceptable for operation in dual vertical and horizontal polarizations but is considerably more stringent for circularly polarized applications. © 2011 Wiley Periodicals, Inc. *Microwave Opt Technol Lett* 53:1435–1439, 2011; View this article online at wileyonlinelibrary.com. DOI 10.1002/mop.26016

Key words: polarization; evanescent-mode filters; ridged waveguide filters; bandpass filters; computer-aided design; tolerance analysis

1. INTRODUCTION

The demands for modern microwave filters are manifold and include properties such as wide bandwidth, improved out-of-band performance, the ability to generate transmission zeros, and preservation of all polarizations.

To preserve the polarization of signals, two approaches are commonly applied: first, the entire waveguide circuit is rotationally symmetric, e.g. Refs. 1 and 2; secondly, components require a common center axis, and every cross-section must be two-plane symmetric. Examples of the second class are wideband orthogonal-mode horn applications [3, 4] and quadruple-ridged waveguide components [5, 6]. Both approaches benefit from extended bandwidth, e.g., Refs. 1 and 3, as only those modes that satisfy structural symmetry along with that of the incoming signal are excited.

A polarization-preserving quadruple-ridged waveguide quasi-lowpass filter is presented in Ref. 6 for millimeter-wave applications. As structural dimensions are small in that frequency range, the request for two additional quadruple-ridged waveguide impedance transformers for matching purposes does not significantly increase the size of the overall component. However, in the 10 GHz range, waveguide filters need to be compact to comply with small overall system requirements.

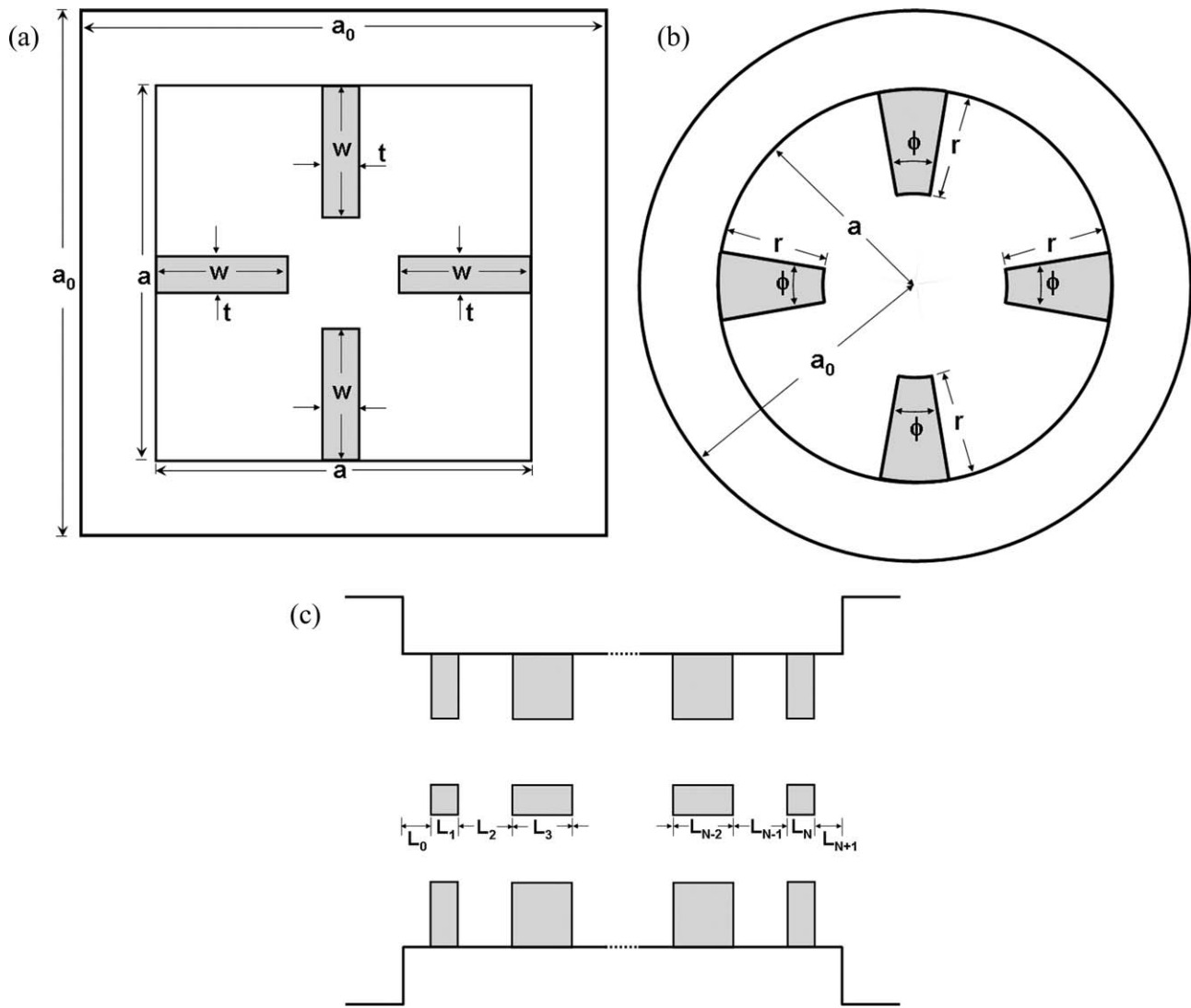


Figure 1 (a) Cross-sections of square polarization-preserving evanescent-mode filter. (b) Cross sections of circular polarization-preserving evanescent-mode filter. (c) Longitudinal view

Therefore, this article focuses on polarization-preserving filter designs using an evanescent-mode technique which is well known for its compactness compared to regular waveguide filters, e.g. Refs. 7–9. Two such designs are presented for 9.5 GHz applications, one in square and one in circular waveguide technology [10].

2. DESIGN GUIDELINES

Figure 1 shows the cross-sections of the polarization-preserving evanescent-mode filters in square [Fig. 1(a)] and circular [Fig. 1(b)] waveguide technologies along with their longitudinal view [Fig. 1(c)]. Note that the ridges in the circular structure are of a shape that is defined in the circular coordinate system. This is a common approach in circular waveguide technology [10–12].

For the computations of scattering parameters, the mode-matching technique (MMT) is used to characterize individual discontinuities. The quadruple-ridged waveguide sections, which act as filter resonators, are solved by a recently developed eigenvalue mode-spectrum analysis (EMA) [13] that determines the cutoff frequencies and coupling matrix to the adjacent evanescent-mode waveguide. Although an arbitrary number of ridges and ridge placements are allowed within this technique [13], they are set here to produce quadruple-ridged sections to comply with the polarization-preserving properties of the filters. In the

absence of such a numerical technique, the design engineer can resort to using commercially available electromagnetic field solvers that include or can be linked to an optimization scheme.

The design of the polarization-preserving evanescent-mode filters proceeds as follows:

1. Select square or circular input/output ports that are in accordance with the frequency range of operation. For the 9.5 GHz examples shown in this article, we chose a square WR75 and a circular WC94 waveguide (Table 1).

TABLE 1 Dimensions (in mm) of Polarization-Preserving Evanescent-Mode Filters According to Figure 1

	Figure 4	Figure 5
a_0	19.050	11.9126
a	10.000	7.000
Ridges	$w = 4.02, t = 1.0$	$r = 5.5, \phi = 9.0^\circ$
$L_0 = L_8$	0.000	1.231
$L_1 = L_7$	1.810	1.446
$L_2 = L_6$	9.141	10.720
$L_3 = L_5$	4.100	3.181
L_4	9.275	11.571

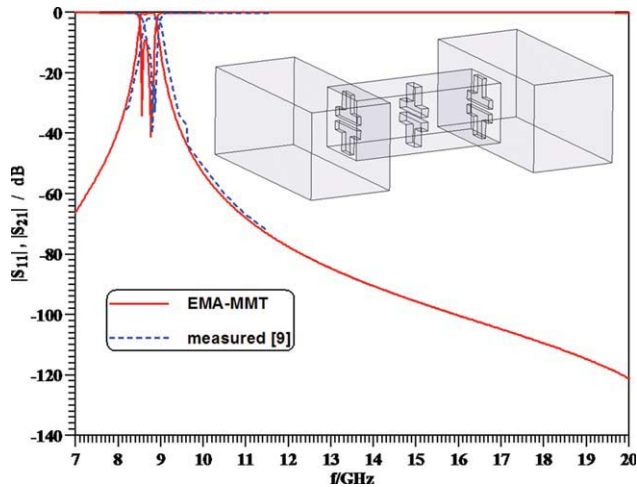


Figure 2 Validation of EMA-MMT code in Cartesian coordinates; performance of a three-pole 9 GHz T-septum evanescent-mode filter presented in Ref. 9. [Color figure can be viewed in the online issue, which is available at wileyonlinelibrary.com]

2. Design the evanescent-mode waveguide and the thickness and extension (gap width) of ridges. The evanescent-mode waveguide must operate below cutoff over the bandwidth of the filter. The ridges are chosen such that the fundamental-mode cutoff frequency is in close to that of the input/output guides. This step requires an iterative process as a compromise must be reached between the difference of the sizes of the two hollow guides, the gap width, and the thickness of the ridges. The minimum housing dimensions of the evanescent-mode waveguide is that for which the optimization (in step 4) produces zero lengths for L_0 and L_{N+1} [Fig. 1(c)].
3. Select the number N of resonators and initial lengths L_0 to L_{N+1} . This can be achieved by a rigorous technique, e.g. Ref. 14, or by selecting values from previously published (not necessarily polarization-preserving) evanescent-mode filters, e.g. Refs. 7–9, and 11.
4. Fine-optimize (e.g., Ref. 15) the section lengths in Fig. 1(c) to yield a filter performance within a prescribed margin of return and insertion loss. Note that all cross-sections remain identical in this step and, therefore, need to be solved only once. The number of optimization parameters is reduced by the symmetry of section lengths (c.f. Table 1).

3. VALIDATION

This section serves to validate the computed results obtained from the electromagnetic software codes [13]. The first example is a three-pole evanescent-mode T-septum filter presented in Ref. 9. This model fits the general prescription of four ridges in a rectangular waveguide operated below cutoff although it is not a polarization-preserving filter. Figure 2 shows the results obtained with the combination of the EMA-MMT when compared to measurements [9]. Very good agreement is observed except for the poor measured return loss as explained in Ref. 9. Note also that in this example, the input/output ports support the TE_{30} mode beyond 20 GHz, but it does not influence the filter behavior until 28 GHz where both the fundamental TE_{10} and the TE_{30} modes create the next passband (c.f. Ref. 9).

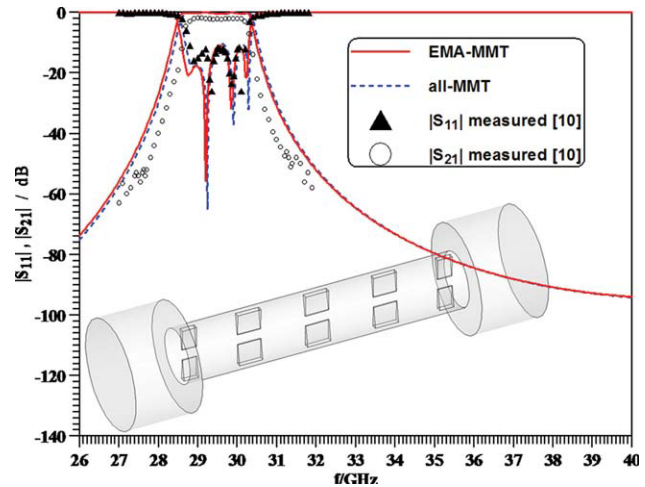


Figure 3 Validation of EMA-MMT code in circular-cylindrical coordinates; performance of a five-pole 30 GHz dual-ridge evanescent-mode filter presented in Ref. 10. [Color figure can be viewed in the online issue, which is available at wileyonlinelibrary.com]

The second example is a five-pole dual-ridged circular waveguide evanescent-mode filter presented in Ref. 10 with structural dimensions obtained from Ref. 11. Figure 3 shows a comparison between the eigenvalue technique used here, an all-radial MMT analysis and measurements from Refs. 10 and 11. Very good agreement is again observed, with the reduction in measured bandwidth attributed to the manufacturing process as outlined in Ref. 10.

4. RESULTS

Following the guidelines presented in Section 2, we introduce two design examples of polarization-preserving evanescent-mode filters. The specifications were set for a fourth-order filter with a midband frequency of 9.5 GHz, a bandwidth of 500 MHz, and 20 dB return loss.

Figure 4 (solid lines) shows the performance of the first example using square waveguide technology. The dimensions are specified in Table 1. It is noted that the first and last section

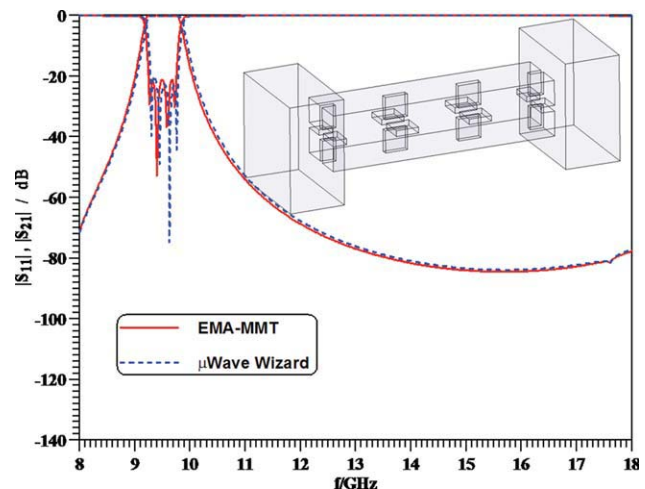


Figure 4 Performance of a polarization-preserving evanescent-mode filter in square waveguide technology (dimension; c.f., Fig. 1 and Table 1) and comparison with results of μ Wave Wizard. [Color figure can be viewed in the online issue, which is available at wileyonlinelibrary.com]

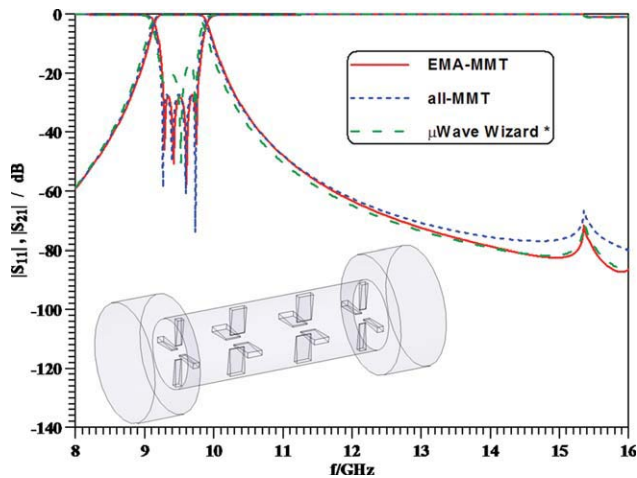


Figure 5 Performance of a polarization-preserving evanescent-mode filter in circular waveguide technology (dimension; c.f., Fig. 1 and Table 1) and comparison with results of an all-MMT code and μ Wave Wizard (* note that μ Wave Wizard uses rectangular ridges of cross-section $1.098 \times 5.075 \text{ mm}^2$). [Color figure can be viewed in the online issue, which is available at wileyonlinelibrary.com]

lengths vanish, thus indicating that the aperture of the evanescent-mode guide is enough to facilitate coupling from the input guide to the first quadruple-ridge resonator. For comparison, we show the results obtained with the commercial software package μ Wave Wizard as dotted lines in Figure 4. Excellent agreement is obtained, thus verifying the design parameters specified in Table 1. Note that the little dip in the two curves at 17.6 GHz (and in subsequent figures) signals the cutoff frequency of the next higher-order mode excited in the feeding waveguide.

The same specifications are used for the design of a polarization-preserving evanescent-mode filter in circular waveguide technology. The performance is shown in Figure 5 as solid lines and shows excellent agreement with the results of the all-MMT code (dotted lines) used in Figure 3. The third set of curves is that obtained with the μ Wave Wizard. The differences are attributed to the fact that the conical ridge sections are replaced by rectangular ones. Following the conversion given in Ref. 16, the

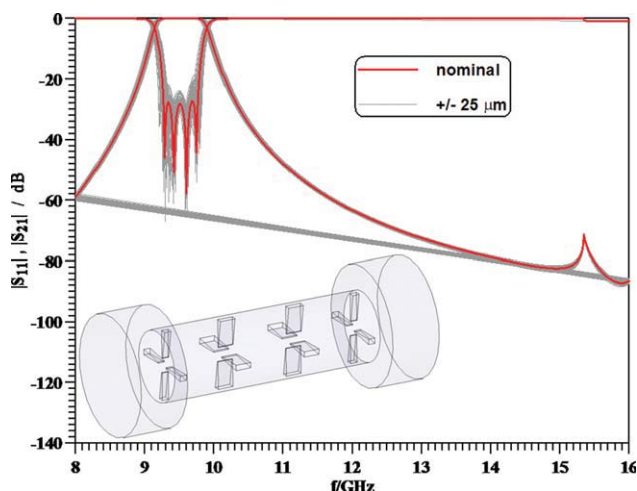


Figure 6 Tolerance analysis (100 trials) of the filter in Figure 5 with $\pm 25 \mu\text{m}$ variations in structural dimensions. [Color figure can be viewed in the online issue, which is available at wileyonlinelibrary.com]

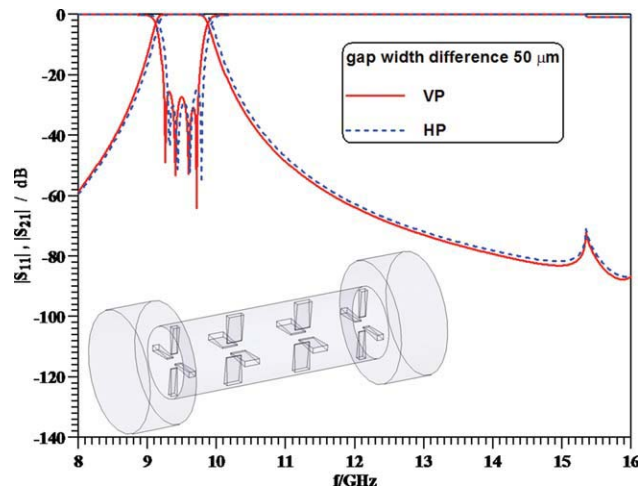


Figure 7 Performance of the filter in Figure 5 if the vertical and horizontal gap widths of ridges [c.f., Fig. 1(b)] differ by $50 \mu\text{m}$. [Color figure can be viewed in the online issue, which is available at wileyonlinelibrary.com]

ridge thickness is 1.098 mm, and parameter r in Table 1 is adjusted to 5.075 mm.

One of the controversial issues related to evanescent-mode filters is their perceived sensitivity to tolerances in the manufacturing process, especially so as they are more compact than traditional direct-coupled waveguide filters. Therefore, Figure 6 shows a tolerance analysis of the filter presented in Figure 5. (For details on filter tolerances, the reader is referred to Ref. 17.) One hundred trials with manufacturing tolerances of $\pm 25 \mu\text{m}$, which is usually accepted in waveguide-based circuits, are shown as thin grey lines together with the thick solid lines indicating the optimized values. The nearly horizontal lines are caused by the trace back from the last point of trial i to the first point of trial $i + 1$. The tolerances include all (asymmetric) section lengths, the radius of the evanescent-mode waveguide, and the thickness and gap width of the ridges. Only the two-plane symmetry in the cross-section is maintained. Compared to the sensitivity of other waveguide filters [17], the behavior displayed in Figure 6 is normal and thus should not raise concerns of fabrication sensitivity. It is noted that the frequency shift is due to variations in the cross-section whereas section-length changes mostly influence the return loss.

Another issue of practical importance is a possible deviation from the two-plane symmetry. Therefore, Figure 7 shows performances for the two polarizations under the assumption that the horizontal gap width ($2a - 2r$) in Figure 1(b) is $50 \mu\text{m}$ larger than the vertical one. Obviously, the influence on the transmission coefficients is negligible. However, due to the slight frequency shift, the overall bandwidth covering both vertical (VP) and horizontal (HP) polarizations is reduced by approximately 50 MHz, which is acceptable for dual linear polarization if the filter design takes such a bandwidth reduction into consideration.

The situation changes completely, although, if the filter is operated in circular polarization. The two transmission coefficients shown in Figure 7 come with a difference of almost 20° in their phases (not shown here) due to the $50 \mu\text{m}$ differences in vertical and horizontal gap widths. This leads to an axial ratio of approximately 3 dB which is unacceptable in most applications. After specifying a maximum axial ratio of 0.5 dB, a reverse calculation of tolerances leads to a maximum difference

of 8 μm between the vertical and horizontal gap widths. Thus the compactness of the filter—if indeed applied for circular polarization—comes at the price of high manufacturing accuracy.

5. CONCLUSIONS

Evanescent-mode filters formed by quadruple ridge sections in rectangular and circular waveguides provide a compact solution for applications involving both filtering and polarization preservation of input signals. Design guidelines are provided and require availability of a commercial (or other) electromagnetic field solver. The method used in this work is validated by measurements. Performances and dimensions of square and circular waveguide filters operating at 9.5 GHz are presented and validated. A sensitivity analysis performed for the circular filter reveals normal dependence on manufacturing tolerances if dual linear, i.e., horizontal and vertical polarization is envisaged. However, due to sensitivity on the transmission phases, tolerances for circular polarization are tighter.

ACKNOWLEDGMENT

This work was supported by the Natural Sciences and Engineering Research Council of Canada.

REFERENCES

1. A.D. Olver, P.J.B. Clarricoats, A.A. Kishk, and L. Shafai, Microwave horns and feeds, IEEE Press, New York, 1994.
2. S. Amari and J. Bornemann, Design of polarization-preserving circular waveguide filters with attenuation poles, Microwave Opt Technol Lett 31 (2001), 334–336
3. G.L. James, P.R. Clark, and K.J. Greene, Diplexing feed assembly for application to dual-reflector antennas, IEEE Trans Antennas Propag 51 (2003), 1024–1029
4. H.Z. Zhang, A wideband orthogonal-mode junction using a junction of a quad-ridged coaxial waveguide and four ridged sectoral waveguides, IEEE Microwave Wireless Compon Lett 12 (2002), 172–174
5. W. Sun and C.A. Balanis, Analysis and design of quadruple-ridged waveguides, IEEE Trans Microwave Theory Tech 42 (1994), 2201–2207
6. F.M. Vanin, E.J. Wollack, K. Zaki, and D. Schmitt, Polarization-preserving quadruple-ridge waveguide filter and four-fold symmetric transformer, In: 2006 IEEE MTT-S Int Microwave Symp Dig, San Francisco, USA, June 2006, pp. 127–140.
7. G. Craven and C.K. Mok, The design of evanescent mode waveguide band-pass filters for a prescribed insertion loss characteristic, IEEE Trans Microwave Theory Tech 19 (1974), 295–308
8. H.F. Chappell, Waveguide low pass filter using evanescent mode inductors, Microwave J 21 (1978), 71–72
9. V.A. Labay and J. Bornemann, CAD of T-septum waveguide evanescent-mode filters, IEEE Trans Microwave Theory Tech 41 (1993), 731–733
10. U. Balaji and R. Vahldieck, Mode-matching analysis of circular-ridged waveguide discontinuities, IEEE Trans Microwave Theory Tech 46 (1998), 191–195
11. U. Balaji, Field theory analysis and design of circular waveguide components, Ph.D. dissertation, University of Victoria, Victoria, BC, Canada, 1997.
12. A. Morini, T. Rozzi, and A. Angeloni, Accurate calculation of the modes of the circular multiridge waveguide, IEEE MTT-S Int Microwave Symp Dig, Denver, CO, June 1997, pp. 199–202.
13. S.Y. Yu and J. Bornemann, Classical eigenvalue mode-spectrum analysis of multiple ridged rectangular and circular waveguides for the design of narrowband waveguide components, Int J Numer Model 22 (2009), 395–410

14. S. Amari, J. Bornemann, and R. Vahldieck, A technique for designing ring and rod dielectric resonators in cutoff waveguides, Microwave Opt Technol Lett 23 (1999), 203–205
15. K. Madsen, H. Schaer-Jacobsen, and J. Voldby, Automated mini-max design of networks, IEEE Trans Circuits Systems CAS-22 (1975), pp. 791–796.
16. J. Bornemann, S. Amari, J. Uher, and R. Vahldieck, Analysis and design of circular ridged waveguide components, IEEE Trans Microwave Theory Tech 47 (1999), 330–335
17. J. Bornemann, U. Rosenberg, S. Amari, and R. Vahldieck, Tolerance analysis of bypass-, cross- and direct-coupled rectangular waveguide bandpass filters, IEEE Proc Microwave Antennas Propag 152 (2005), 167–170

© 2011 Wiley Periodicals, Inc.

TIME-DOMAIN AUGMENTED EFIE AND ITS MARCHING-ON-IN-DEGREE SOLUTION

Yan Shi^{1,2} and Jian-Ming Jin²

¹School of Electronic Engineering, Xidian University, Xi'an, China; Corresponding author: shiyan@mail.xidian.edu.cn

²Center for Computational Electromagnetics, Department of Electrical and Computer Engineering, University of Illinois at Urbana-Champaign, Urbana, IL

Received 23 August 2010

ABSTRACT: A time-domain augmented electric field integral equation (TDAEFIE) and its marching-on-in-degree (MOD) solution are presented for analysis of transient electromagnetic responses from three-dimensional closed conducting bodies of arbitrary shape. By enforcing a condition on the normal component of the electric flux density, the TDAEFIE eliminates the potential internal resonance problem of the time-domain electric field integral equation (TDEFIE) algorithm. With the use of weighted Laguerre polynomials as entire-domain temporal basis functions, the MOD solution overcomes the late-time instability problem that often occurs in the marching-on-in-time (MOT) approach. Compared with the MOD solution of the time-domain combined field integral equation (TDCFIE), the MOD solution of the TDAEFIE is more efficient because it takes less computational time for calculating the matrix elements and the matrix-vector multiplications related to the excitation at the right-hand side of the matrix equation. Numerical results are presented to illustrate the good performance of the TDAEFIE algorithm. © 2011 Wiley Periodicals, Inc. Microwave Opt Technol Lett 53:1439–1444, 2011; View this article online at wileyonlinelibrary.com. DOI 10.1002/mop.26015

Key words: time-domain augmented electric field integral equation; marching-on-in-degree; marching-on-in-time; time-domain combined field integral equation

1. INTRODUCTION

Analysis of transient electromagnetic phenomena has received increased attention because of various engineering applications such as design of broadband antennas, analysis of nonlinear circuits, and simulation of electromagnetic interference problems. Numerical techniques for analyzing transient problems can be classified into time-domain techniques based on integral and differential equations. Because of the use of spatial volume discretization, differential equation-based techniques are preferred for transient electromagnetic simulation of inhomogeneous structures. However, integral equation-based techniques are more efficient for analysis of problems consisting of perfect electrical conductors and piecewise homogeneous media.